SYNTHESIS AND PROPERTIES OF INORGANIC COMPOUNDS

Low-temperature synthesis and luminescent properties of lanthanum metaphosphate LaP_3O_9 : Tb

M. V. Belobeletskaya[a], N. I. Steblevskaya[a], M. A. Medkov[a]

[a]*Institute of Chemistry of the Far Eastern Branch of the Russian Academy of Sciences, Vladivostok, 690022 Russia*

**e-mail: rita@ich.dvo.ru*

Received August 17, 2024
Revised October 03, 2024
Accepted October 03, 2024

Promising for inorganic luminophores, terbium-doped lanthanum metaphosphates $La_{1-x}Tb_xP_3O_9$ (x = 0.05, 0.1, 0.2, 0.3, 0.4) were synthesised by extraction-pyrolytic method at low temperature in comparison with known methods. The crystal structure and optical properties of the obtained samples were characterised by X-ray phase analysis, IR and luminescence spectroscopy, and the unit cell parameters were calculated. Compounds having rhombic structure, pr. gr. C 222_1, were obtained in the temperature range of 500-900ºC. All parameters of the unit cell decrease linearly with the introduction of terbium into lanthanum metaphosphate. $La_{1-x}Tb_xP_3O_9$ compounds show intense luminescence in the region of 450 - 650 nm. The $La_{0.8}Tb_{0.2}P_3O_9$ sample obtained in one hour annealing at pyrolysis temperature of 900ºC shows maximum luminescence intensity.

Keywords: lanthanum metaphosphates, terbium, doping, luminescence

DOI: 10.31857/S0044457X250103e4

INTRODUCTION

The development of methods for the synthesis of new chemically, thermally and mechanically stable materials with optical properties is a pressing task.High heat resistance, as well as chemical and radiation resistance of materials based on rare earth element phosphates (**REE**) determine the prospects of their use as matrices for phosphors[1–6].

Based on luminescent materials containing REE ions, plasma panels, light-emitting diodes, fluorescent lamps, liquid crystal displays, and temperature sensors have been created [7 – 10]. In recent years, phosphate luminophore materials have

attracted great attention due to the relative simplicity of synthesis, high stability and low toxicity [11]. Thus, interest in further study of phosphates is due to their unique properties and wide range of applications.

The most commonly used methods for synthesizing REE metaphosphates are the solid-phase method [12–16] , precipitation from solutions [7, 17–19] and the sol-gel method [16, 20] .

Traditional high-temperature solid-phase synthesis is most frequently used [12–16] . When using this method, REE oxides are thoroughly ground, mixed with a phosphorus-containing reagent, and fired several times at different temperatures, with the final firing temperature reaching 800 – 1200°C, each stage of the process taking from several hours to days. Phosphorus(V) oxide, ammonium or alkali metal dihydrogen phosphates or hydrogen phosphates are used as sources of phosphate ions. Depending on the reaction temperature, phosphorus-containing reagents sometimes should be taken in excess to compensate for losses caused by sublimation. The solid-phase method has several disadvantages: multiple stages, long duration, and high synthesis temperature.

The production of REE phosphates, including doped ones, is very often carried out from aqueous solutions containing ammonium phosphates or phosphoric acid, with phosphates of various compositions being synthesized depending on the temperature and reaction conditions [17]. In studies [7, 18, 19] REE metaphosphates were successfully obtained by precipitation from solutions. At the same time, dehydration of the obtained precursors was carried out at a temperature of 100 – 110 °C for 10 – 12 hours, and firing at a temperature of 900 – 1000°C was required to obtain the final metaphosphate.

When using the sol-gel method for the synthesis of rare earth metaphosphates [16, 20], the transparent sol formed at low temperature was heated at a higher temperature, converting it into a viscous gel from which the final product is formed at the optimal temperature.

However, compared to precipitation and solid-state reactions, this method is used less frequently due to the lengthy and complex process. For example, in work [16], yttrium metaphosphate was obtained from anhydrous phosphorus oxide P_2O_5 in a mixture with yttrium and europium chlorides in isopropanol. In the first stage, yttrium and europium alkoxides were synthesized, after which anhydrous phosphorus oxide P_2O_5 powder was added to them with intensive stirring for ~6 h to obtain a transparent solution of heterometallic alkoxides. After that, the sol was hydrolyzed by adding excess water, resulting in the formation of a transparent gel, which was dried at 80°C to obtain a white xerogel. The latter was calcined at temperatures from 80 to 1200°C for 5 h. Since the synthesized yttrium and europium alkoxides actively react with water vapor contained in the air, all experiments were carried out in a dry argon atmosphere at all stages of the process.

Since the preparation method determines the morphology, particle size, composition, and luminescent properties of materials, the search for new methods for the synthesis of phosphate phosphors remains a relevant topic of scientific research [20, 21].

This paper presents the results of studying the synthesis conditions and luminescent properties of terbium-doped lanthanum metaphosphates using the extraction-pyrolytic method, which has not been previously used for this purpose.

EXPERIMENTAL PART

For the synthesis of lanthanum metaphosphates LaP_3O_9: Tb, saturated extracts of lanthanum and terbium were used. To obtain the extracts, nitrate solutions containing 0.012 mol/L of lanthanum and 6.6×10^{-3} mol/L of terbium were used as the aqueous phase; the pH value of the aqueous phase at 7.0-7.5 was created by adding an aqueous solution of ammonia. The pH value of the aqueous phase was controlled using a pH-meter/millivoltmeter Mark-901. REE extraction was carried out with mixed solutions of 1.95 mol/L acetylacetone and 0.0167 mol/L 1,10-phenanthroline in benzene. The

organic and aqueous phases in a ratio of 1:1 were intensively mixed at room temperature for 30 minutes on a mechanical shaker SK-30 (Korea). The composition of the REE aqueous phases was controlled before and after extraction using a Shimadzu AA 7000 atomic absorption spectrophotometer. The concentration of La and Tb in organic extracts was determined by the L-lines of the characteristic spectrum using energy-dispersive X-ray fluorescence analysis on a Shimadzu EDX-800HS instrument. The excitation source was an X-ray tube with a Rh-anode, the measurement time was 100 s. The calculation of element concentrations was carried out using a calibration graph with the instrument software. For the synthesis of LaP_3O_9: Tb, tributyl phosphate was added to the saturated extracts in a molar ratio of Ln : P = 1 : 4, terbium was introduced into the lanthanum extract in various ratios. Homogeneous saturated extracts were evaporated at 60-80°C until paste formation and subjected to pyrolysis at various temperatures in a muffle furnace for 1-2 hours.

X-ray analysis of the samples was carried out on a D8 Advance BrukerAXS diffractometer (Germany) in Cu K_α-radiation using the EVA search program with the PDF-2 powder data bank. Luminescence excitation and luminescence spectra of the phosphors were recorded at 300 K on a Shimadzu RF-5301 PC spectrofluorimeter. IR spectra of the samples were recorded at room temperature on a Vertex 70 instrument in the range of 4000-400 cm^{-1}.

RESULTS AND DISCUSSION

Various phosphors based on ortho- and metaborates, oxysulfides, polyphosphates, polyniobates, and polytantalates of REE have previously been successfully synthesized by the extraction-pyrolytic method [21-23].

REE metaphosphates crystallize in two structural types. For elements of the La–Eu series, the orthorhombic crystal system is characteristic, while lanthanides with a small ionic radius (Ln = Gd–Lu, Y) have monoclinic symmetry [11, 12]. The first reflections corresponding to the orthorhombic phase of lanthanum metaphosphate

appear already at a pyrolysis temperature of 400°C (Fig. 1, curve *1*). At a temperature of 500°C, a phase of crystalline lanthanum metaphosphate LaP_3O_9 of orthorhombic modification (space group $C222_1$ (20), a = 11.303, b = 8.648, c = 7.397 Å, α = 90°, β = 90°, γ = 90°, Z = 4, $V_{unit\ cell}$ = 723.044 Å^3) [6, 24] is formed (Fig. 1, curve *2*). In the temperature range of 500–900°C, the crystallinity of the samples increases while the composition remains unchanged. With an increase in temperature to 1000°C and above, the metaphosphate begins to decompose, and an additional phase of lanthanum orthophosphate $LaPO_4$ of monoclinic modification appears.

According to [1], all oxygen atoms in the LaP_3O_9 matrix are tetrahedrally bonded to phosphorus atoms. Phosphorus ions occupy two different crystallographic positions and form two types of PO_4 tetrahedra. One tetrahedron has good symmetry, while the other is asymmetric. The PO_4 tetrahedra share corners, forming one-dimensional spiral chains along the *c* axis, connected to each other by Ln–O bonds. The La atom is coordinated by eight oxygen atoms, forming a slightly distorted dodecahedron [17, 19], resulting in La–O bond lengths ranging from 2.415 to 2.749 Å, with the nearest La–La distance being 4.315 Å, and the distance between chains is approximately 7 Å [24].

X-ray diffraction patterns of terbium-doped lanthanum metaphosphates $La_{1-x}Tb_xP_3O_9$ (x = 0.05; 0.10; 0.20; 0.30; 0.40) are presented in Fig. 2. With the addition of terbium in amounts up to 20 mol. %, no impurity peaks appear on the diffraction pattern of the orthorhombic modification of LaP_3O_9 (Fig. 2, curves *1* , *2*). As can be seen from Table 1, which presents the unit cell parameters for $La_{1-x}Tb_xP_3O_9$, with an increase in Tb^{3+} concentration up to 20 mol. %, all unit cell parameters tend to decrease linearly with increasing dopant concentration.

As previously noted, La^{3+} ions in LaP_3O_9 occupy only one crystallographic position, forming LaO_8 dodecahedra, and since the ionic radius of Tb^{3+} is smaller than that of La^{3+} [12, 25], the unit cell parameters will decrease, indicating the substitution of La^{3+} ions by Tb^{3+} ions.

In compounds $La_{1-x}Tb_xP_3O_9$ (x = 0.30, 0.40), a second phase of terbium metaphosphate TbP_3O_9 of monoclinic modification appears (space group $P2_1/c$ (14), a = 11.258, b = 20.220, c = 10.138 Å, α = 90°, β = 97.150°, γ = 90°, Z = 12, $V_{unit\ cell}$ = 2289.835 Å^3) (Fig. 2, curves *3* , *4*). In the structure of TbP_3O_9, rare-earth ions are located inside slightly distorted TbO_6 octahedra, isolated from each other by PO_4 tetrahedra [11, 16].

Table 2 presents the IR spectral data of lanthanum metaphosphates. When LaP_3O_9 is doped with Tb^{3+} ions, no changes in the IR spectra of the compounds are observed.

In the IR spectra, absorption bands at 1271 and 1153 cm^{-1} are attributed to symmetric stretching vibrations ν_s(O–P–O) and asymmetric vibrations ν_{as}(O–P–O), respectively. The absorption band at 1120 cm^{-1} can be assigned to asymmetric stretching vibrations ν_{as}(O–P–O). Additionally, the spectrum shows absorption bands at 567 and 532 cm^{-1} related to bending vibrations δ(O–P–O). Absorption bands at 499, 474 and 457 cm^{-1} can be attributed to bending vibrations characteristic of (P–O–P) groups [20, 26]. Absorption bands at 682 and 771 cm^{-1} correspond to symmetric stretching vibrations, while bands at 950, 1006 and 1053 cm^{-1} to asymmetric vibrations of (P–O–P) groups . The observed bands are consistent with a structure consisting of an infinite chain of tetrahedral P–O bonds.

The luminescent characteristics of the obtained $La_{1-x}Tb_xP_3O_9$ metaphosphate samples were evaluated based on luminescence excitation and emission spectra at 300 K, which were recorded under identical conditions.

Figure 3 shows the luminescence excitation spectra of $La_{1-x}Tb_xP_3O_9$ metaphosphates with different Tb^{3+} content, including those obtained at different temperatures. As seen in Fig. 3, the position of bands in the luminescence excitation spectra, recorded at the wavelength of maximum luminescence of the Tb^{3+} ion λ_{em} = 545 nm, does not change for $La_{1-x}Tb_xP_3O_9$ metaphosphates.

In the wavelength range of 220-270 nm, a broad intense band with a maximum at ~241 nm is recorded, which can be attributed to the transition $4f^8 \rightarrow 4f^7 5d^1$ in the Tb

$^{3+}$ion [7, 12, 21, 27]. As the concentration of terbium ions increases up to 20 mol. %, the intensity of this band increases (Fig. 3a, curves *1* , *2*). With further increase in the concentration of terbium ions, the intensity of the $4f^8 \rightarrow 4f^7 5d^1$ transition band decreases (Fig. 3a, curves *3* , *4*).

In the region 300-390 nm at λ_{em} = 545 nm, low-intensity bands are observed, corresponding to transitions from the ground level of the Tb^{3+} $^7F_6$ ion to the excited levels $^5D_0$, $^5D_4$, $^5L_7$, $^5L_9$, $^5G_5$, $^5G_6$ [7, 15, 25].

Fig. 3b shows the luminescence excitation spectrum of the $La_{0.8}Tb_{0.2}P_3O_9$ compound synthesized at different pyrolysis temperatures. With increasing pyrolysis temperature of organic precursors (Fig. 3b), the intensity of the *f–d* transition band of the Tb^{3+} ion increases, reaching a maximum at an annealing temperature of 900°C, which can be explained by the increase in crystallinity of the samples.

Fig. 4 shows the luminescence spectra of the synthesized lanthanum metaphosphates. The luminescence spectra of La_{ex} = 241 nm consist of a series of bands in the region of 450-650 nm, corresponding to transitions between the multiplets $_{1-x}Tb_xP_3O_9$ recorded at an excitation wavelength λ $^5D_4 \rightarrow {}^7F_{6,5,4,3}$, characteristic for the Tb^{3+} ion [7, 12, 21, 27]. At λ_{ex} = 241 nm, the position of the transition bands $^5D_4 \rightarrow {}^7F_{6,5,4,3}$, as well as the intensity distribution across the bands in doped lanthanum metaphosphates $La_{1-x}Tb_xP_3O_9$ remain unchanged with varying concentrations of the doping Tb^{3+} ions. As shown in Fig. 4a, the band at ~547 nm, corresponding to the $^5D_4$–$^7F_5$ transition characteristic of the Tb_{3+} ion, has a maximum intensity.

The highest luminescence intensity, determined by integrating the area under the transition bands $^5D_4 \rightarrow {}^7F_{6,5,4,3}$ in the spectra of $La_{1-x}Tb_xP_3O_9$ samples, is shown by lanthanum metaphosphates containing 20 mol. % Tb^{3+} (Fig. 4b, curve *1*). Increasing the Tb^{3+} ion concentration to 30-40 mol. % leads to a decrease in luminescence intensity, which can be explained by concentration quenching [7, 20, 27]. Additionally, as shown earlier (Fig. 1), in compounds $La_{1-x}Tb_xP_3O_9$ (x = 0.30, 0.40), besides the $La_{1-x}Tb_xP_3O_9$ phase, a monoclinic terbium metaphosphate phase TbP_3O_9 appears. Considering

that the luminescence intensity of TbP_3O_9 is significantly lower than that of terbium-doped lanthanum metaphosphate [12, 21], the appearance of an additional TbP_3O_9 phase in the compound leads to a decrease in the luminescence intensity of $La_{1-x}Tb_xP_3O_9$ at dopant concentrations >30 mol. % .

Increasing the synthesis temperature of $La_{1-x}Tb_xP_3O_9$ metaphosphates to 900°C leads to a sequential increase in the integral luminescence intensity (Fig. 4b, curve *1*), which may be associated with increased crystallinity of the compounds [20, 21]. As shown above, at temperatures >1000°C, lanthanum metaphosphate begins to partially decompose, and a phase of lanthanum orthophosphate appears in the sample composition (Fig. 1, curve *4*). Apparently, the decrease in luminescence intensity with further temperature increase can be explained by the presence of an additional phase of lanthanum orthophosphate, which has lower luminescence intensity [20, 21].

CONCLUSION

The conditions for obtaining orthorhombic lanthanum metaphosphates (space group $C222_1$) were studied using extraction-pyrolytic and low-temperature methods. The influence of pyrolysis temperature on the composition of the obtained metaphosphates was investigated. It was shown that the formation of metaphosphates begins already at 400°C; in the range of 500-900°C, there is an increase in the crystallinity of the samples, and with further temperature increase, the metaphosphates partially decompose to form $LaPO_4$ orthophosphate. Terbium-doped compounds $La_{1-x}Tb_xP_3O_9$ (x = 0.05; 0.10; 0.20; 0.30; 0.40) were synthesized.

The IR spectra of the compounds contain absorption bands characteristic of stretching (457, 474, 499 cm^{-1}) and bending (682 and 771 cm^{-1}) vibrations of the P-O-P bond.

$La_{1-x}Tb_xP_3O_9$ metaphosphates exhibit luminescence in the 450-50 nm range, with the emission maximum at ~545 nm associated with the $^5D_4$ - $^7F_5$ transition in the Tb^{3+} ion. The nature of the spectra does not change with varying terbium concentration. In

the synthesized $La_{1-x}Tb_xP_3O_9$ polyphosphate, the maximum luminescence intensity is observed at a terbium concentration of 20 mol. %.

Thus, the extraction-pyrolytic method is promising for obtaining REE-doped metaphosphates.

FUNDING

The work was carried out within the framework of state assignments of the Institute of Chemistry, Far Eastern Branch of the Russian Academy of Sciences (project No. FWFN (0205)-2022-0001).

CONFLICT OF INTEREST

The authors declare that they have no conflict of interest.

REFERENCES

1. *Zhou C., Dong P., Ga P. et al.* // Spectrochim. Acta, Part A. 2024. V. 313. P. 124102. https://doi.org/10.1016/j.saa.2024.124102

2. *Patel L., Mehta M., Sharma R.* // IJCRT. 2023. V. 11. № 2. P. 444.

3. *Wozniak-Levushkina V. S., Arapova A. A., Spassky D. A. et. al.* // Physics of the Solid State. 2022. V. 64. № 12. P. 1896

4. *Dongyan Y., Xingya W., Gongqin Y. et al.* // Mater. Rev. 2020. V. 34. P. 41.

5. *Baranovskaya V.B., Karpov Yu.A., Petrova K.V. et al.* // Izv. VUZov. Tsvetn. metallurgiya. 2020. № 6. P. 4. https://doi.org/10.17073/0021-3438-2020-6-4-23

6. *Sedov V.A., Glyadelova Ya.B., Asabina E.A. et al.* // Russ. J. Inorg. Chem. 2023. V. 68. № 3. P. 239.

7. *Singh V., Ravita Kaur S. et al.* // Optik. 2021. V. 244. P. 167323. https://doi.org/10.1016/j.ijleo.2021.167323

8. *Fang M-H., Bao Z., Huang W-T. et al.* // Chem. Rev. 2022. V. 122. № 13. P. 11474.

https://doi.org/10.1021/acs.chemrev.1c00952
9. *Farooq M., Rafiq H., Shah A.I. et al.* // ECS J. Solid State Sci. Technol. 2023. V. 12. № 12. P. 126002. https://doi.org/10.1149/2162-8777/ad1062
10. *Krutyak N., Spassky D., Deyneko D.V. et al.* // Dalton Trans. 2022. V. 51. P. 11840.
11. *Zhang X., Chen P., Wang Z. et al.* // Solid State Sci. 2016. V. 58. P. 80. https://doi.org/10.1016/j.solidstatesciences.2016.06.002
12. *Wang Y., Wang D.* // J. Solid State Chem. 2007. V. 180. № 12. P. 3450. https://doi.org/10.1016/j.jssc.2007.10.008
13. *Kononets N.V., Seminko V.V., Maksimchuk P.O. et al.* // Low Temp. Phys. 2017. V. 43. № 8. P. 1009. https://doi.org/10.1063/1.5001311
14. *Yuan J-L., Zhang H., Zhao J-T. et al.* // Opt. Mater. 2008. V. 30. № 9. P. 1369. https://doi.org/10.1016/j.optmat.2007.07.004
15 . *Wu C., Wang Y., Wang D.* // Electrochem. Solid-State Lett. 2008. V. 11. № 2. P. J9. https://doi.org/10.1149/1.2809168
16. *Briche S., Zambon D., Chadeyron G. et al.* // J. Sol-Gel Sci. Technol. 2010. V. 55. P. 41. https://doi.org/10.1007/s10971-010-2211-z
17. *Onishi T., Hatada N., Kuramitsu A. et al.* // J. Cryst. Growth. 2013. V. 380. № 1. P. 78. https://doi.org/10.1016/j.jcrysgro.2013.06.001
18. *Singh V., Yadav A., Rao A.S. et al.* // Optik. 2020. V. 206. P. 164239. https://doi.org/10.1016/j.ijleo.2020.164239
19. *Hachani S., Moine B., El-akrmi A. et al.* // J. Lumin. 2010. V. 130. P. 1774. https://doi.org/ 10.1016/j.jlumin.2010.04.009
20. *Yang J., Jia X., Zeng X. et al.* // J. Mater. Sci. 2015. V. 50. P. 4405. https://doi.org/10.1007/s10853-015-8996-y
21. *Steblevskaya N.I., Belobeletskaya M.V., Medkov M.A.* Phosphors based on rare and rare earth metal oxides: extraction-pyrolytic synthesis and properties. Functional ceramic and composite materials for practical applications: synthesis, properties, application. Vladivostok: VVGU Publishing House, 2022. 240 p.

https://doi.org/10/12466/0677-0-2022

22. *Steblevskayaa N. I., Belobeletskaya M. V.* // Theor. Found. Chem. Eng. 2023. V. 57. № 5. P. 1192. https://doi.org/10.1134/S0040579523050317

23. *Steblevskayaa N. I., Belobeletskaya M. V.* // Russ. J. Inorg. Chem. 2023. V. 68. № 7. P. 913.

24. *Matuszewski J., Kropiwnicka J., Znamierowska T.* // J. Solid State Chem. 1988. V. 75. P. 285.

25. *Bugaenko L.T., Ryabykh S.M., Bugaenko A.L.* // Moscow University Chemistry Bulletin. 2008. V. 49. № 6. P. 363.

26. *Nakamoto K* . Infrared and Raman Spectra of Inorganic and Coordination Compounds: Part A – Theory and Applications in Inorganic Chemistry. N.-Y.: John Wiley and Sons, 2009.

27. *Blasse G., Grabmaier B.C* . Luminescent materials. Berlin: Springer-Verlag, 1994. 233 p.

Table 1. Unit cell parameters of doped lanthanum metaphosphates

Sample	*a* , Å	*b* , Å	*c* , Å ^{3}	*wRp* , %	*V* , Å ^{3}
$La_{0.95}Tb_{0.05}P_3O_9$	11.286(2)	8.632(2)	7.377(1)	4.12	714.776
$La_{0.9}Tb_{0.1}P_3O_9$	11.247(2)	8.600(2)	7.347(1)	5.71	710.633
$La_{0.8}Tb_{0.2}P_3O_9$	11.206(3)	8.574(2)	7.313(3)	6.84	702.635

Table 2. Band assignments in IR spectra of doped lanthanum metaphosphates

LaP_3O_9 $La_{1-x}Tb_xP_3O_9$	Assignment
457 474	δ(POP)
499 532 567	δ(OPO)
682 771	ν_s(POP)
950 1006 1053	ν_{as}(POP)
1271 1153 1120	ν_s(OPO) ν_{as}(OPO)

FIGURE CAPTIONS

Fig. 1. X-ray diffraction patterns of LaP_3O_9, obtained at 400 (*1*), 500 (*2*), 900 (*3*) and 1100°C (*4*).

Fig. 2. X-ray diffraction patterns of samples with composition $La_{0.9}Tb_{0.1}P_3O_9$(*1*), $La_{0.8}Tb_{02}P_3O_9$(*2*), $La_{0.7}Tb_{0.3}P_3O_9$(*3*), $La_{0.6}Tb_{0.4}P_3O_9$(*4*).

Fig. 3. Luminescence excitation spectra of $La_{1-x}Tb_xP_3O_9$ samples at x = 0.05 (*1*), 0.1 (*2*), 0.2 (*3*), 0.3 (*4*), 0.4 (*5*), obtained at 900°C (a), and $La_{0.8}Tb_{0.2}P_3O_9$ sample obtained at 700 (*1*), 800 (*2*) and 900°C (*3*); λ_{em} = 545 nm, 300 K (b).

Fig. 4. Luminescence spectra of $La_{1-x}Tb_xP_3O_9$ at x = 0.05 (*1*), 0.1 (*2*), 0.2 (*3*), 0.3 (*4*), 0.4 (*5*), obtained at 900°C (a); dependence of compounds luminescence intensity on precursor annealing temperature (*1*) and Tb^{3+} ion concentration (*2*); λ_{ex} = 241 nm, 300 K (b).

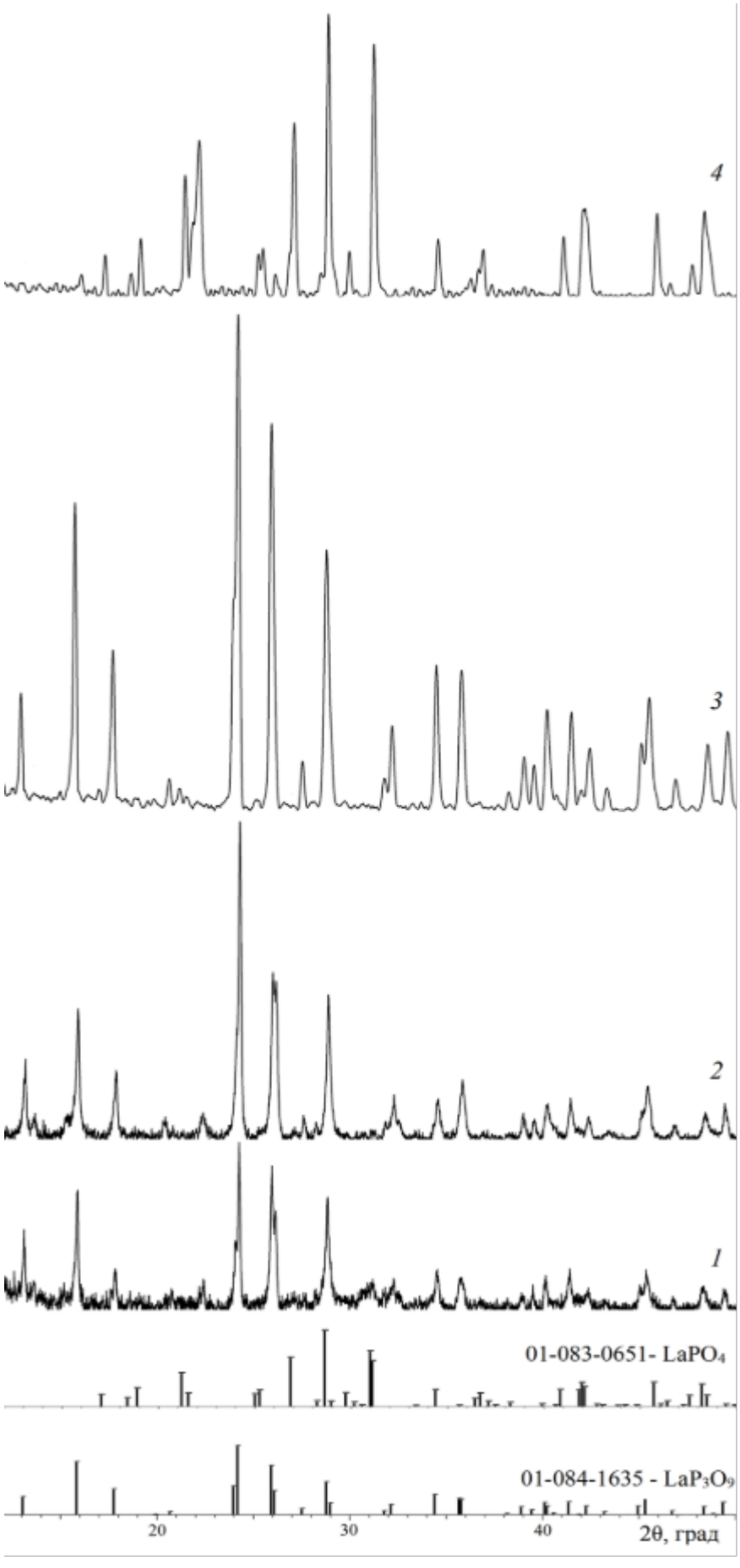
4
3
2
1
01-083-0651- LaPO4
01-084-1635 - LaP3O9
20
30
40
2θ, град

Fig. 1

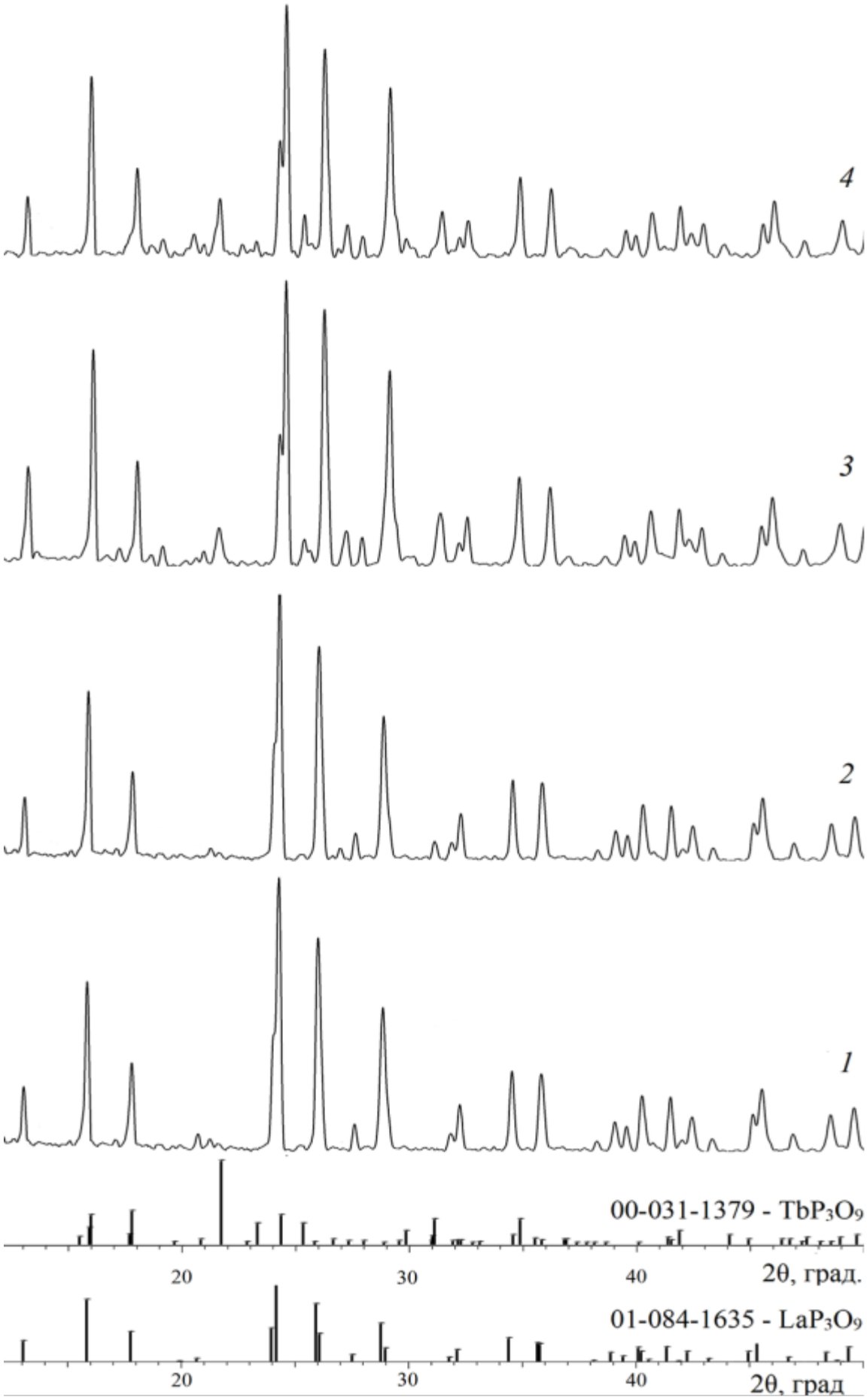
4
3
2
1
00-031-1379 - TbP3O9
20
30
40
2θ, град.
01-084-1635 - LaP3O9
20
30
40
2θ, град

Fig. 2.

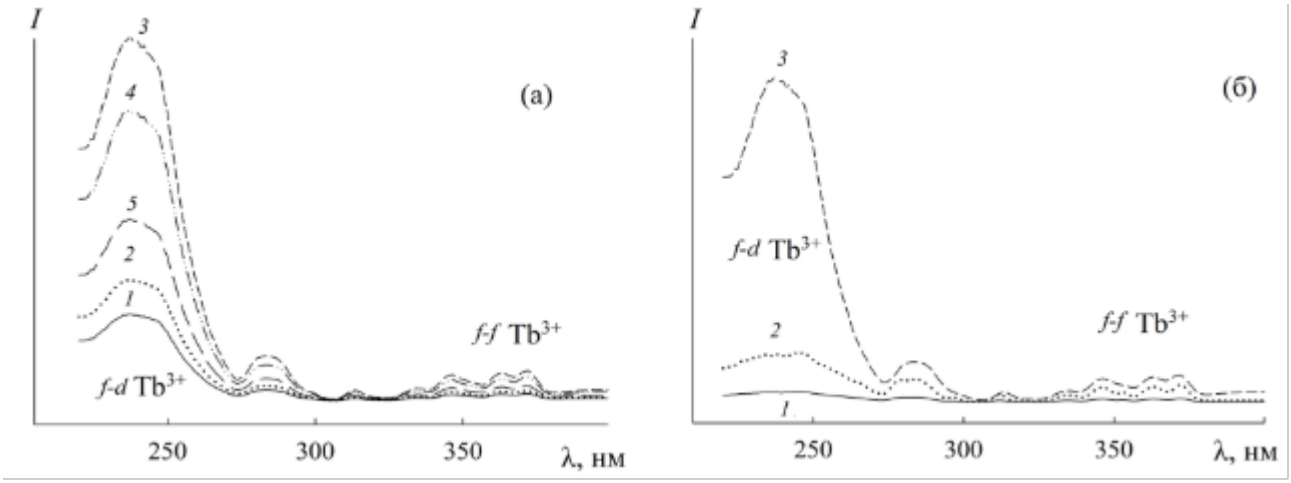

Fig. 3. I,

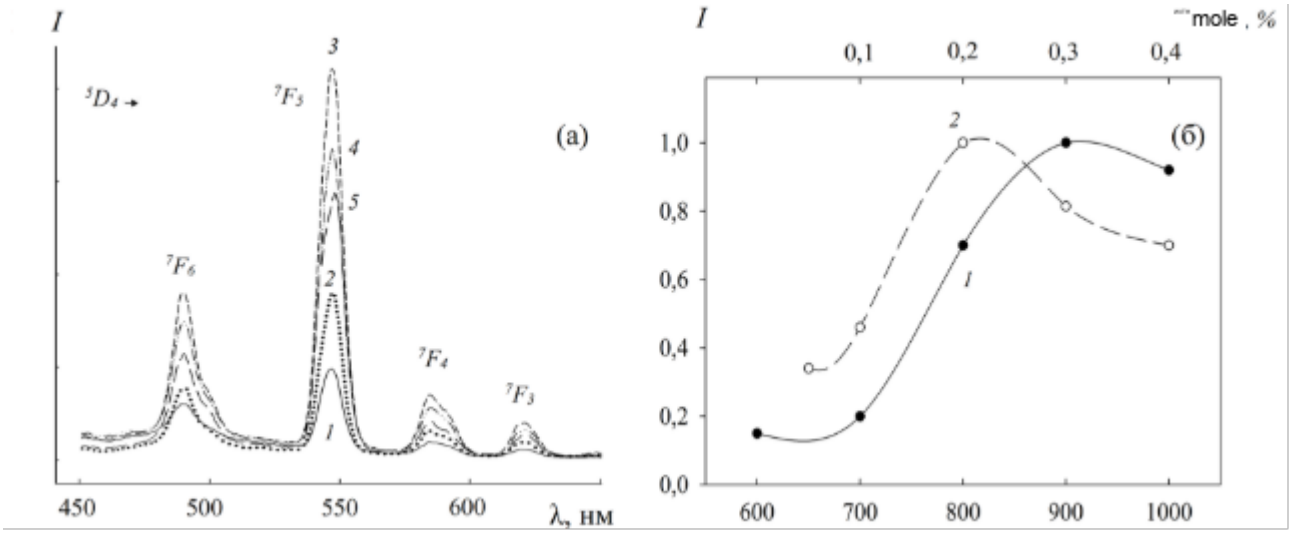

Fig. 4.